Acta Crystallographica Section C
Crystal Structure Communications
ISSN 0108-2701

Aripiprazole salts. I. Aripiprazole nitrate

Eleonora Freire,[a]*‡ Griselda Polla[b] and Ricardo Baggio[b]*

[a]Gerencia de Investigación y Aplicaciones, Centro Atómico Constituyentes, Comisión Nacional de Energía Atómica and Escuela de Ciencia y Tecnología, Universidad Nacional General San Martín, Buenos Aires, Argentina, and [b]Gerencia de Investigación y Aplicaciones, Centro Atómico Constituyentes, Comisión Nacional de Energía Atómica, Buenos Aires, Argentina
Correspondence e-mail: freire@tandar.cnea.gov.ar, baggio@cnea.gov.ar

Received 26 January 2012
Accepted 12 March 2012
Online 16 March 2012

The crystal structure of aripiprazole nitrate (systematic name: 4-(2,3-dichlorophenyl)-1-{4-[(2-oxo-1,2,3,4-tetrahydroquinolin-7-yl)oxy]butyl}piperazin-1-ium nitrate), $C_{23}H_{28}Cl_2N_3O_2^+\cdot NO_3^-$ or $AripH^+\cdot NO_3^-$, is presented and the molecule compared with the aripiprazole molecules reported so far in the literature. Bond distances and angles appear very similar, except for a slight lengthening of the C—NH distances involving the protonated N atom, and the main differences are to be found in the molecular spatial arrangement (revealed by the sequence of torsion angles) and the intermolecular interactions (resulting from structural elements specific to this structure, *viz*. the nitrate counter-ions on one hand and the extra protons on the other hand as hydrogen-bond acceptors and donors, respectively). The result is the formation of [100] strips, laterally linked by weak π–π and C—Cl$\cdots\pi$ interactions, leading to a family of undulating sheets parallel to (010).

Comment

Aripiprazole (7-{4-[4-(2,3-dichlorophenyl)piperazin-1-yl]butoxy}-1,2,3,4-tetrahydroquinolin-2-one, Arip) is an antipsychotic drug, perhaps the most relevant representative of a modern family of atypical antipsychotics (Travis *et al.*, 2005), with a therapeutic activity which is different from the classical antipsychotic drugs in standard use.

Regarding the forms in which Arip appears, the drug crystallizes in a number of different polymorphic and solvatomorphic forms, including an amorphous phase, described in a large number of patents, which indicates the commercial importance of the drug. However, and as expected in this type of documentation, the structural information provided is far from complete: the compounds appear to be poorly characterized, and when their X-ray powder diffraction (XRPD) diagrams are reported, they usually fulfil the role of fingerprint identifiers. Only a few of these compounds have been studied from a structural point of view and included in the public domain as entries in the Cambridge Structural Database (CSD; Allen, 2002). The main source of this information is the paper by Tessler & Goldberg (2006), complemented by two excellent works by Braun *et al.* (2009*a*,*b*). In the Braun *et al.* (2009*a*) work, a number of different forms of the Arip molecule in its free form are reported and are in the CSD with refcodes MELFIT01 [hereafter B; in what follows, independent Arip molecules, either in the same or in different structures, will be named with uppercase letters), MELFIT02 (C), MELFIT03 (D and E: one single structure, two independent molecules), MELFIT04 (F and G: one single structure, two independent molecules) and MELFIT05 (H). The Braun *et al.* (2009*b*) publication deals with different solvates: MELFEP01 (ethanol solvate, A), MELFOZ01 (methanol solvate, I), MELFUF01 (monohydrate, J) and MOXDAF01 (1,2-dichloroethane solvate, K).

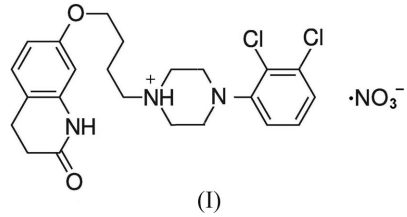

(I)

There are also numerous patents describing Arip salts, basically derived from carboxylic acids (for example, Brand *et al.*, 2007; Pongo *et al.*, 2009), but none of these present structural information despite the fact that such a study might

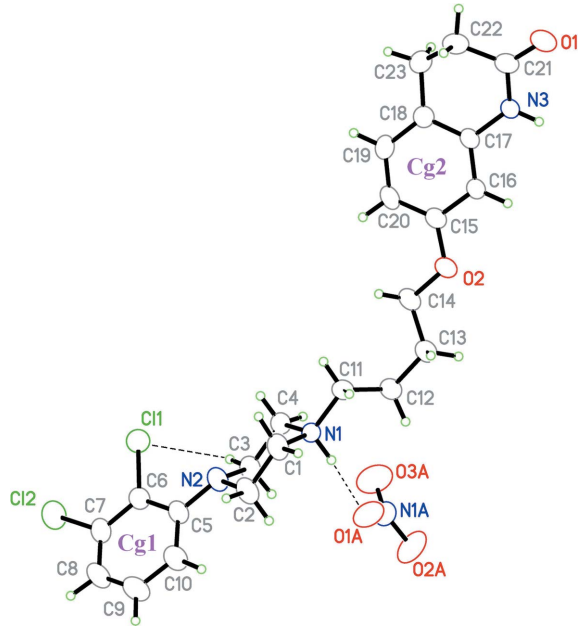

Figure 1
The molecular structure of (I), with displacement ellipsoids drawn at the 40% probability level, showing the asymmetric unit, together with atom and centroid labelling. Some relevant hydrogen-bond interactions are shown as dashed lines.

‡ Member of Consejo Nacional de Investigaciones Científicas y Técnicas, Conicet.

  doi:10.1107/S0108270112010785

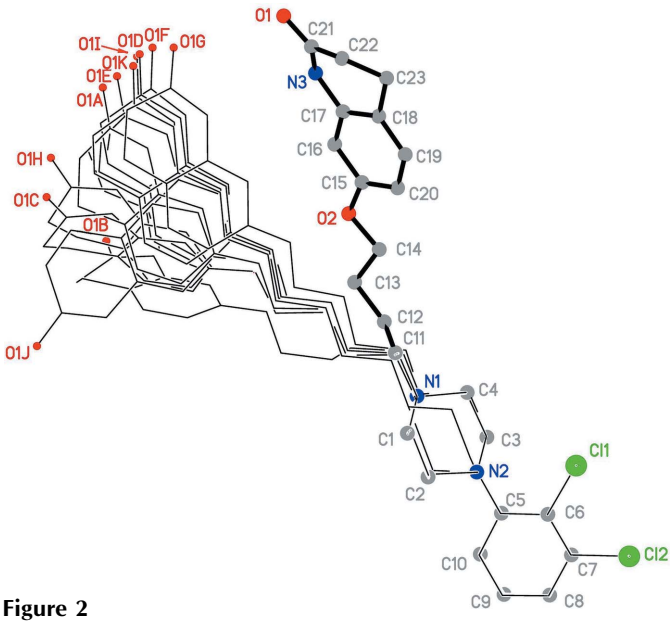

Figure 2
A comparison of the conformation of (I) (heavy lines) with the different Arip molecules reported in the literature (thin lines). Structural codes (A–K) are defined in the *Comment*.

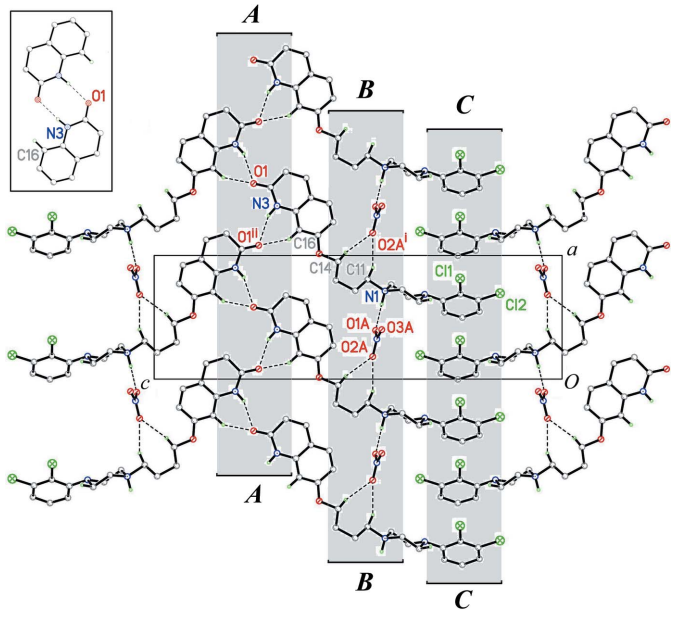

Figure 3
Packing diagram of (I), showing a projection down [100]. The shaded *A*, *B* and *C* regions correspond to different hydrogen-bonding regimes, as discussed in the *Comment*. Inset: the centrosymmetric diamide $R_2^2(8)$ dimer present in structures A, D, E, H, I and K. [Symmetry codes: (i) $x+1$, y, z; (ii) $x-\frac{1}{2}$, y, $-z+\frac{3}{2}$.]

deserve due attention; there are many examples of pharmaceutical drugs which are being delivered as salts, due to solubility or stability considerations. We present herein the crystal structure of aripiprazole nitrate, $AripH^+\cdot NO_3^-$, (I), the first of an intended series on aripiprazole salts obtained from inorganic or organic acids.

Fig. 1 shows an atomic displacement ellipsoid plot of the asymmetric unit of (I), consisting of an $AripH^+$ cation and an NO_3^- counter-ion providing for charge balance. The $AripH^+$ cation is metrically similar to Arip in the many polymorphs and solvatomorphs already reported and disclosed above, the only difference being the protonation of N1. This analogy is reflected in Table 1 which compares bond distances in (I) with the mean values of all the reported molecules (A–K): the general similarities are apparent, as well as the lengthening of the bonds involving the N1 atom, due to protonation.

More significant differences are detectable in the way the molecular groups evolve in space. Fig. 2 shows a fitting of (I) and the remaining 11 structures of the A–K group. A similar comparison has already been made in Braun *et al.* (2009*a*) involving the different polymorphs of the free base reported therein.

The present comparison was made by forcing the best fit of the dichlorophenyl–piperazine region of the Arip molecules, ending up with a reasonable fit in that specific region for all 12 cases, with 11 of them bunching in the mid-region and structure (I) clearly evolving away from the bulk. From a strictly formal point of view, this is explained by the torsion angles in the N1···C13 region of J being distinctly different from those of the other structures, as can be seen in Table 2. The reasons for this should be looked for in the fact that it is in the $N1^+$ neighbourhood where the structural differences arise, and this will be apparent when discussing the hydrogen-bonding scheme.

Intermolecular interactions defining the spatial arrangement are of variable type and strength. Table 3 presents the more significant hydrogen bonds, while Table 4 complements this with the remaining π–π and Cl···π contacts. The first entry in Table 3 corresponds to an intramolecular C—H···Cl interaction characteristic for the dichlorophenyl–piperazine group in all reported Arip variants (Fig. 1), being in (I) rather unexceptional. In addition, the present structure lacks any significant intermolecular C—H···Cl contacts, contrasting with many reported Arip compounds where the terminal Cl atoms are acceptors for these types of interactions (see, for instance, Braun *et al.*, 2009*a*). Fig. 3 shows an extended view of a [010] projection, along the medium-length axis, where three definite regions are clearly defined by their unique interactions and presented as shaded columns (*A*, *B* and *C*). Regions *A* and *B* are determined by the hydrogen bonds appearing in Table 3 as entries 2 and 3 on one side and entries 4, 5 and 6 on the other, and both define broad strips running along [100].

The first of these interactions, the strong N3—H3···O1($x-\frac{1}{2}$, y, $-z+\frac{3}{2}$) hydrogen bond between amide groups of adjacent Arip molecules, is common to most of the reported Arip variants, the sole exception being monohydrated species J (CSD refcode MELFOZ01) where they are (surprisingly) absent. One explanation for the situation in J is the presence of a water molecule of solvation which acts as an acceptor for the N3—H3 donor. Thus, in the packing organization of J, the solvent water (disordered by symmetry) serves as an acceptor for the N3—H3 donor, thus blocking this interaction site and dramatically changing the whole subsequent three-dimensional arrangement.

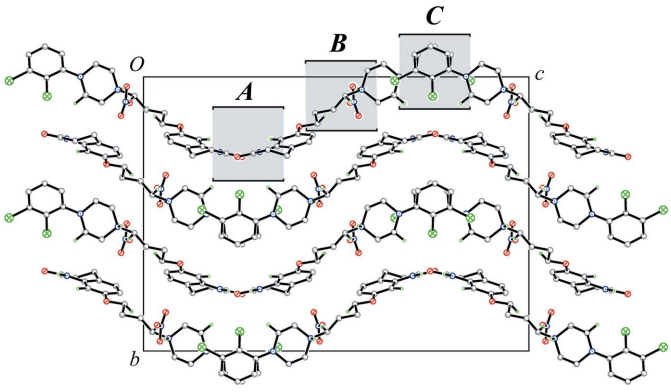

Figure 4
Packing diagram of (I) projected along [010], perpendicular to the view shown in Fig. 3.

In all the remaining cases, the interactions do exist, and result in one of two well defined supramolecular synthons. The first, much more frequent, synthon is a centrosymmetric diamide $R_2^2(8)$ dimer, shown as an inset in Fig. 3, and occurring in all those Arip variants crystallizing in $P\overline{1}$, *viz*. structures A, D, E, H, I and K. The second synthon is a catemer, and appears only in structures B, C and H, which crystallize in space groups with a 2_1 axis running along a short cell dimension, and which serves for the 'threading' of the resulting $R_2^1(6)$ loops (for graph-set nomenclature, see Bernstein *et al.*, 1995). The present case, (I), corresponds to this latter class of catemers, as seen in column *A* in Fig. 3. There is, however, a substantial difference in that the symmetry element responsible for the chain formation is in this case the *a*-glide plane instead of a 2_1 axis.

In contrast with the common character of the previous interaction, the second group (restricted to zone *B*) is more unique to the present structure (I), as some of the main structural elements (the nitrate counter-ion as an acceptor and the extra H1 proton as a donor) are specific to this structure, and even if the strips are common construction bricks for most Arip structures, in the present case, this second interaction strengthens their mutual link and enhances their internal cohesion, to form a rather different entity (Fig. 3). The [100] strips are in turn laterally linked by the weak nonconventional π–π and C—Cl$\cdots\pi$ interactions presented in Table 4, and isolated in zone *C* (Fig. 3). The result is a family of parallel sheets shown laterally in Fig. 4, where their undulating character can clearly be appreciated. The intersheet separation is $b/4$ = *ca* 4.95 Å, and their mutual interaction is accordingly weak, mainly due to C—H$\cdots\pi$ interactions (in Table 3, entries 7 and 8, not shown in Fig. 4).

Finally, the results presented herein confirm some expected results, *viz*. that the protonated state of AripH$^+$ and the inclusion of a strong hydrogen-bond acceptor (the required counter-anion) must necessarily introduce interesting new structural properties, which are frequently associated with new physical (and sometimes commercially useful) properties. Accordingly, with these expectations, further work is in progress.

Experimental

Aripiprazole (1.5×10^{-4} mol, 67 mg) was dissolved in a boiling mixture of methanol (5 ml) and acetone (0.5 ml). When dissolution was complete, an excess of HNO_3(c) was added dropwise and the resulting solution left to cool. Excellent quality crystals of AripH$^+\cdot$NO$_3^-$, in the form of colourless prisms, appeared within a few hours, and these were used as obtained without further recrystallization.

Crystal data

$C_{23}H_{28}Cl_2N_3O_2^+\cdot NO_3^-$
M_r = 511.39
Orthorhombic, *Pbca*
a = 8.4644 (2) Å
b = 19.8264 (5) Å
c = 27.9406 (7) Å
V = 4688.9 (2) Å^3
Z = 8
Mo *K*α radiation
μ = 0.32 mm^{-1}
T = 295 K
0.38 × 0.24 × 0.20 mm

Data collection

Oxford Diffraction Gemini CCD S Ultra diffractometer
Absorption correction: multi-scan (*CrysAlis PRO*; Oxford Diffraction, 2009)
T_{min} = 0.91, T_{max} = 0.94
48362 measured reflections
5809 independent reflections
4721 reflections with $I > 2\sigma(I)$
R_{int} = 0.027

Refinement

$R[F^2 > 2\sigma(F^2)]$ = 0.042
$wR(F^2)$ = 0.103
S = 1.09
5809 reflections
419 parameters
All H-atom parameters refined
$\Delta\rho_{max}$ = 0.26 e Å^{-3}
$\Delta\rho_{min}$ = −0.35 e Å^{-3}

Table 1
Comparative bond lengths (Å).

Bond	*d* (I)	⟨*d* (A–K)⟩†
Cl1—C6	1.7241 (16)	1.728 (8)
Cl2—C7	1.7325 (17)	1.736 (14)
O1—C21	1.225 (2)	1.228 (6)
O2—C14	1.4261 (19)	1.415 (40)
O2—C15	1.3683 (19)	1.374 (12)
N1—C1	1.493 (2)	1.453 (10)
N1—C4	1.501 (2)	1.458 (4)
N1—C11	1.505 (2)	1.464 (14)
N2—C2	1.457 (2)	1.459 (6)
N2—C3	1.471 (2)	1.464 (9)
N2—C5	1.418 (2)	1.413 (7)
N3—C17	1.4083 (19)	1.410 (7)
N3—C21	1.353 (3)	1.351 (8)
C1—C2	1.509 (3)	1.514 (8)
C3—C4	1.513 (2)	1.509 (10)
C5—C6	1.404 (2)	1.405 (12)
C5—C10	1.397 (2)	1.389 (9)
C6—C7	1.389 (2)	1.383 (20)
C7—C8	1.385 (3)	1.371 (18)
C8—C9	1.372 (3)	1.372 (16)
C9—C10	1.382 (3)	1.383 (12)
C11—C12	1.514 (2)	1.517 (19)
C12—C13	1.528 (2)	1.514 (34)
C13—C14	1.501 (3)	1.497 (30)
C15—C16	1.391 (2)	1.381 (12)
C15—C20	1.387 (2)	1.375 (11)
C16—C17	1.383 (2)	1.379 (11)
C17—C18	1.397 (2)	1.391 (7)
C18—C19	1.381 (2)	1.379 (14)
C18—C23	1.504 (2)	1.507 (10)
C19—C20	1.393 (3)	1.385 (15)
C21—C22	1.503 (3)	1.496 (11)
C22—C23	1.520 (3)	1.492 (23)

† This column reports the unweighted average value of equivalent distances in the A–K group (as defined in the *Comment*), with the usual standard deviation from the average shown in parentheses.

Table 2
Comparison of selected torsion angles (°).

	(I)	A	B	C	D	E	F	G	H	I	J	K
T1	−84.5 (2)	−167.3 (4)	−159.4 (8)	−168.1 (6)	−159.9 (8)	−167.5 (3)	−173.1 (3)	−156.1 (3)	−164.9 (4)	−171.1 (3)	−73.6 (3)	−167.1 (4)
T2	−169.6 (1)	60.2 (7)	178.0 (9)	173.0 (6)	174.2 (8)	169.4 (3)	−179.6 (3)	−170.6 (3)	173.4 (4)	168.0 (3)	−171.1 (2)	173.7 (4)
T3	−69.0 (2)	174.7 (6)	−173.3 (9)	−175.9 (7)	−161.8 (9)	−176.5 (3)	−178.3 (9)	−169.6 (3)	−175.6 (4)	−175.4 (3)	172.8 (2)	−177.8 (4)

Torsion angle codes: T1 = C4—N1—C11—C12, T2 = N1—C11—C12—C13 and T3 = C11—C12—C13—C14.

Table 3
Hydrogen-bond geometry (Å, °).

*Cg*2 is the centroid of the C15–C20 ring.

D—H···*A*	*D*—H	H···*A*	*D*···*A*	*D*—H···*A*
C3—H3*A*···Cl1	0.97 (2)	2.58 (2)	3.217 (2)	124 (2)
N1—H1···O1*A*	0.90 (2)	1.89 (2)	2.778 (2)	176 (2)
C11—H11*B*···O2*A*^{i}	0.95 (2)	2.40 (3)	3.258 (2)	150 (2)
C14—H14*B*···O2*A*^{i}	0.96 (2)	2.49 (2)	3.429 (2)	165 (2)
N3—H3···O1^{ii}	0.86 (2)	2.18 (2)	2.996 (2)	158 (2)
C16—H16···O1^{ii}	0.96 (2)	2.47 (2)	3.219 (2)	136 (2)
C2—H2*B*···*Cg*2^{iii}	0.96 (2)	2.92 (2)	3.720 (2)	142.6 (14)
C4—H4*A*···*Cg*2^{iv}	0.93 (2)	2.84 (2)	3.534 (2)	132.6 (14)

Symmetry codes: (i) $x+1, y, z$; (ii) $x-\frac{1}{2}, y, -z+\frac{3}{2}$; (iii) $-x+2, -y+1, -z+1$; (iv) $x-\frac{1}{2}, -y+\frac{1}{2}, -z+1$.

Table 4
π–π and Cl–π contacts (Å, °) for (I).

c.c.d. is the centre-to-centre distance, c.p.d. is the centre-to-plane distance and s.a. is the slippage angle (angle subtended by the intercentroid vector to the plane normal). *Cg*1 is the centroid of the C5–C10 ring. For details, see Janiak (2000).

Group 1/group 2	c.c.d. (Å)	c.p.d. (Å)	s.a. (°)
*Cg*1···*Cg*1^{i}	4.238 (2)	3.456 (2)	35.37
Cl1···*Cg*1^{i}	3.404 (2)	3.339 (2)	11.27

Symmetry code: (i) $\frac{1}{2}+x, y, \frac{1}{2}-z$.

All H atoms were found in a difference map and their positions and isotropic displacement parameters were refined freely [methylene C—H = 0.93 (2)–0.96 (2) Å, aromatic C—H = 0.94 (2)–1.01 (3) Å and N—H = 0.87 (2)–0.95 (2) Å].

Data collection: *CrysAlis PRO* (Oxford Diffraction, 2009); cell refinement: *CrysAlis PRO*; data reduction: *CrysAlis PRO*; program(s) used to solve structure: *SHELXS97* (Sheldrick, 2008); program(s) used to refine structure: *SHELXL97* (Sheldrick, 2008); molecular graphics: *SHELXTL* (Sheldrick, 2008); software used to prepare material for publication: *SHELXL97* and *PLATON* (Spek, 2009).

The provision of aripiprazole by Laboratorios Maprimed is gratefully acknowledged. The authors also acknowledge ANPCyT (project No. PME 2006–01113) for the purchase of the Oxford Gemini CCD diffractometer and the Spanish Research Council (CSIC) for provision of a free-of-charge licence to the Cambridge Structural Database (Allen, 2002).

Supplementary data for this paper are available from the IUCr electronic archives (Reference: QS3012). Services for accessing these data are described at the back of the journal.

References

Allen, F. H. (2002). *Acta Cryst.* B**58**, 380–388.
Bernstein, J., Davis, R. E., Shimoni, L. & Chang, N.-L. (1995). *Angew. Chem. Int. Ed. Engl.* **34**, 1555–1573.
Brand, M., Shookrun, M., Gribun, I., Adin, I., Iustain, C., Arad, O. & Kaspi, J. (2007). US Patent 20071837331.
Braun, D. E., Gelbrich, T., Kahlenberg, V., Tessadri, R., Wieser, J. & Griesser, U. (2009*a*). *J. Pharm. Sci.* **98**, 2010–2026.
Braun, D. E., Gelbrich, T., Kahlenberg, V., Tessadri, R., Wieser, J. & Griesser, U. (2009*b*). *Cryst. Growth Des.* **9**, 1054–1065.
Janiak, C. (2000). *J. Chem. Soc. Dalton Trans.* pp. 3885–3896.
Oxford Diffraction (2009). *CrysAlis PRO*. Oxford Diffraction Ltd, Yarnton, Oxfordshire, England.
Pongo, L., Simig, G., Dancso, A. & Morovjan, G. (2009). US Patent 20090111829.
Sheldrick, G. M. (2008). *Acta Cryst.* A**64**, 112–122.
Spek, A. L. (2009). *Acta Cryst.* D**65**, 148–155.
Tessler, L. & Goldberg, I. (2006). *J. Inclusion Phenom. Macrocycl. Chem.* **55**, 255–261.
Travis, M. J., Burns, T., Dursun, S., Fahy, T., Frangou, S., Gray, R., Haddad, P. M., Hunter, R., Taylor, D. M. & Young, A. H. (2005). *Int. J. Clin. Pract.* **59**, 485–495.